TABLE I. Absolute photoelectric cross sections in barns per atom.

Element	Present experimental value	Interpolated value
Pb	76.5 ±4.6	78.6
Sn	10.2 ±0.6	10.6
Ag	7.65±0.46	7.97

because the weighing of the foils is done on an electrical balance. The error involved in the determination of the photoelectron number is found to be about 3.3%. The error in the estimation of the gamma intensity is found to be about 5%. Therefore, the effective error (root-mean-square value) involved in the final photoelectric cross section is about ±6%.

RESULTS

The present experimental values along with the standard interpolated values are given in Table I. It can be seen that the values are in good agreement with the interpolated values within the range of experimental errors.

ACKNOWLEDGMENTS

The authors are thankful to the Department of Atomic Energy, Government of India, Trombay, India for sponsoring this work in the Laboratories for Nuclear Research Andhra University, Waltair, India, and for awarding to one of them (K. P.) a senior scientific assistantship.

PHYSICAL REVIEW VOLUME 142, NUMBER 1 FEBRUARY 1966

Hyperfine Structure of the Stable Lithium Isotopes. I*

RICHARD G. SCHLECHT† AND DOUGLAS W. MCCOLM
Lawrence Radiation Laboratory, University of California, Berkeley, California
(Received 28 June 1965)

The atomic-beam magnetic-resonance technique was used to determine the hyperfine-structure separations and the hyperfine-structure anomaly between the isotopes Li^6 and Li^7 in the $^2S_{1/2}$ ground state. The separated-oscillatory-field method of Ramsey was used to determine the hyperfine-structure separations. The hfs of Li^6 is $\Delta\nu_6=228.20528(8)$ Mc/sec, and of Li^7 is $\Delta\nu_7=803.50404(48)$ Mc/sec. By means of these values and the value for the ratio of the g_I's obtained by Klein, the hyperfine-structure anomaly was determined to be $\Delta_{67}=+1.065(6)\times10^{-4}$. The errors quoted are four times the statistical errors.

I. INTRODUCTION

THE hyperfine-structure separations and anomaly of Li^6 and Li^7 in their $^2S_{1/2}$ ground state have been measured[1] with the atomic-beam magnetic-resonance technique. In 1949 Kusch and Mann[2] measured the hyperfine-structure anomaly of Li^6 and Li^7, using the hyperfine-structure measurements of Kusch and Taub,[3] and obtained $\Delta_{67}=+1.25(27)\times10^{-4}$. Our experiment was undertaken to remeasure Δ_{67} to greater precision. The significance of our result is related to the distribution of nuclear magnetism within the nuclei of Li^6 and Li^7, and is discussed in Part II.[4]

II. APPARATUS AND METHOD

The atomic-beam apparatus used in this experiment, recently built at Berkeley, is described briefly in Sec. IIA and shown in Fig. 1. The distances between the important components and the oven slit are given in Table I.

A. Beam Production and Detection

The lithium beam was produced by heating a stainless steel oven by electron bombardment. A 100-mil iridium ribbon in an oxygen atmosphere of 1×10^{-6} mm of Hg was used as a surface-ionization detector.

For the Li^7 hyperfine-structure determination, the beam was chopped by a mechanical flag driven by a 15-cps oscillator. The output of this oscillator and the signal from the detector were fed into a phase-sensitive amplifier. For the Li^6 hyperfine-structure determination, the radio-frequency current which produced the transitions was modulated at 15 cps instead.

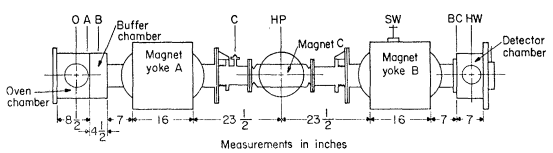

FIG. 1. Diagrammatic sketch of the atomic-beam machine. The oven is at O, entrance slits at A, potassium oven at B, collimator at C, hairpin at HP, stopwire at SW, exit slits at BC, and detector at HW.

* This work was supported in part by the U. S. Atomic Energy Commission and in part by the U. S. Navy.
† Present address: Westinghouse Research Laboratories, Pittsburgh, Pennsylvania.
[1] R. Schlecht, D. McColm, and I. Maleh, Bull. Am. Phys. Soc. 7, 604 (1962).
[2] P. Kusch and A. K. Mann, Phys. Rev. **76**, 707 (1949).
[3] P. Kusch and H. Taub, Phys. Rev. **75**, 1477 (1949).
[4] Douglas McColm, following paper, Phys. Rev. **142**, 14 (1966).

TABLE I. Distances between pertinent parts of atomic-beam machine B and the oven slit.

Part	Distance from oven slit (in.)
A collimator and beam chopper	3
Buffer calibration oven	6
C collimator	42.5
Radio-frequency hairpin	54
Stopwire	85
B collimator	101
Surface ionization detector	104
Foil detector	109

B. Radio-Frequency System

The radio-frequency current was fed into a hairpin constructed of two shorted parallel 4- by-4-in. silver-plated copper plates. The lithium beam passed along the surface of one of the plates and the constant magnetic field H_0 was perpendicular to the plates. As the beam passed either edge of the copper plate, it entered a region where the magnetic field of the radio-frequency signal was parallel to H_0. The edges of the hairpin then gave rise to the separated oscillatory fields that are necessary to produce a Ramsey pattern.[5–7] This system is shown in Fig. 2.

The advantage of this arrangement is that the rf magnetic field in each of the separated regions is produced by the same current; the same rf magnetic field lines pass through each. Thus at once the two regions must have opposite phase and equal amplitude. The phase being exactly opposite assures the symmetry of the Ramsey pattern, while the equality of the amplitudes is necessary for it to be comparable in size to the pedestal. Some care must be taken to insure that the hairpin has longitudinal symmetry, but the dependence of the phase on hairpin geometry is much less in this case than it is when separate hairpins are used for the two rf regions. A possible danger to be noted, however, is the production of longitudinal standing waves along the hairpin which can occur when the wavelength is equal to a multiple of the length of the hairpin. This was not the case in this experiment, and the results obtained in the two possible hairpin orientations show that the phase shift is indeed small.

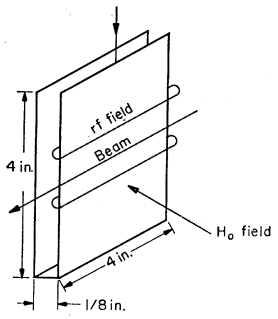

FIG. 2. Radio-frequency hairpin. Two rf magnetic-field lines are indicated.

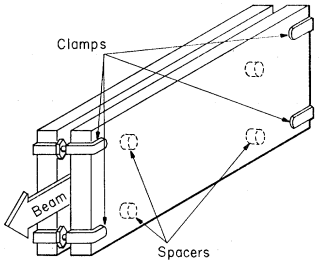

FIG. 3. Hypernom plate assembly, hairpin not shown.

The rf hairpin slid into a $\frac{1}{4}$-in. gap between two parallel plates (each $\frac{1}{2} \times 3 \times 12$ in.) made of a high-permeability material (Westinghouse's Hypernom); the Hypernom plates, which were separated by $\frac{1}{4}$-in. thick quartz spacers and held together with brass clamps, were then placed between the pole tips of a 12-in. electromagnet (Varian V-4012A). By varying the position of the spacers and the pressure on the brass clamps, we could change the homogeneity of H_0. The best homogeneity thus obtained was about 3 parts in 10^5 over the four inches of the hairpin. This system is shown in Fig. 3.

The radio-frequency oscillators were locked with a 10-Mc/sec phase-sensitive detector (Schomandl FDS3 Syncriminator). A 1-Mc/sec crystal oscillator (Manson model RD-140) was used as a standard-frequency source, which was calibrated against an Atomicron. A block diagram of the radio-frequency system used in the Li^6 experiment is shown in Fig. 4. A similar arrangement was used in the Li^7 experiment. When the oscillator was locked to the output of the multiplier, a Lissajous figure appeared on the oscilloscope.

III. THEORY

Lithium has a $^2S_{1/2}$ electronic ground state. The Hamiltonian of an atom with $J=\frac{1}{2}$ in an external magnetic field H_0 is given by

$$\mathcal{H}=-g_J\mu_0\mathbf{J}\cdot\mathbf{H}_0-g_I\mu_0\mathbf{I}\cdot\mathbf{H}_0+[h\Delta\nu/(I+\tfrac{1}{2})]\mathbf{I}\cdot\mathbf{J}, \quad (1)$$

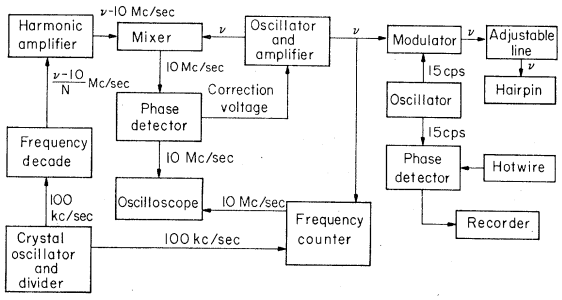

FIG. 4. Block diagram of the radio-frequency system used for the Li^6 hyperfine-structure determination. The surface-ionization detector and electrometer system is called "hotwire."

[5] N. F. Ramsey, Phys. Rev. **76**, 996 (1949).
[6] N. F. Ramsey, Phys. Rev. **78**, 695 (1950).
[7] N. F. Ramsey and H. B. Silsbee, Phys. Rev. **84**, 506 (1951).

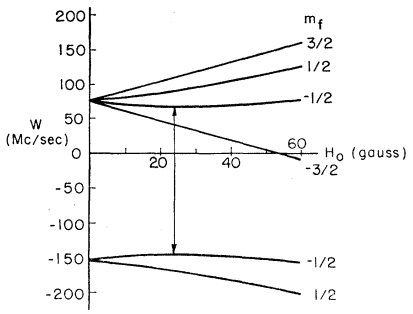

FIG. 5. Breit-Rabi energy-level diagram for Li^6. The $\Delta m_F=0$ field-independent σ transition is indicated by the arrow.

where μ_0 is the value of the Bohr magneton, **I** and **J** are the nuclear and electronic angular momenta, g_I and g_J are the nuclear and electronic g factors, and $\Delta\nu$ is the zero-field hyperfine-structure separation between the $F=I+\frac{1}{2}$ and the $F=I-\frac{1}{2}$ levels. The energy levels of this Hamiltonian are given by the well-known Breit-Rabi formula, which predicts that the field-independent σ transitions, $(F=2,\ m_F=-1)\leftrightarrow(F=1,\ m_F=-1)$ in Li^7 and $(F=\frac{3}{2},\ m_F=-\frac{1}{2})\leftrightarrow(F=\frac{1}{2},\ m_F=-\frac{1}{2})$ in Li^6, occur at the frequency

$$\nu=\nu_{\min}[1+((2I+1)^2/16I)(x-x_{\min})^2], \qquad (2)$$

where

$$\Delta\nu=\nu_{\min}[1-((2I-1)/(2I+1))^2]^{-1/2}, \qquad (3)$$

and

$$x=((g_I-g_J)\mu_0H_0)/h\Delta\nu. \qquad (4)$$

Here μ_0 is the Bohr magneton, $\Delta\nu$ is the hfs separation, and $x_{\min}=(2I-1)/(2I+1)$. These transitions are indicated on Figs. 5 and 6.

By making a least-squares fit of the observed transition frequencies in the neighborhood of the minimum transition frequency to Eq. (2), we obtain the best

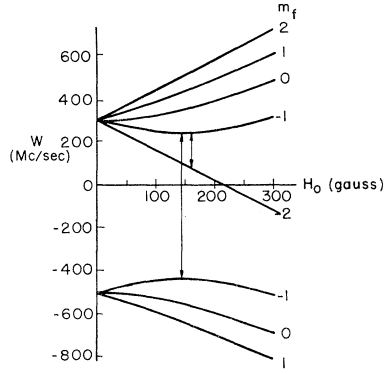

FIG. 6. Breit-Rabi energy-level diagram for Li^7. The $\Delta m_F=0$ field-independent σ transition and the $\sigma m_F=1$ field-calibrating transition are indicated with arrows.

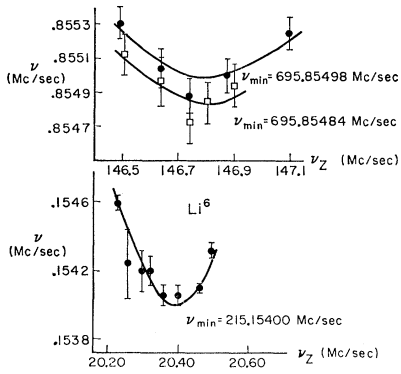

FIG. 7. Li^6 and Li^7 data plots of resonance frequency versus field, and the corresponding least-squares-fit curves. The magnetic field is measured in terms of ν_Z, the frequency of the $F=I+\frac{1}{2}$, $m_F=-I-\frac{1}{2}\leftrightarrow F=I+\frac{1}{2}$, $m_F=-I+\frac{1}{2}$.

value of $\nu_{\min}$, from which we then obtain the hyperfine-structure separation. This scheme has the advantage of not being dependent on the magnetic-field errors to first order.

IV. RESULTS

The experimental data obtained on the Li^7 direct transition are shown in Fig. 7. For this transition two sets of data were obtained, each set being taken for a different orientation of the rf hairpin, to determine the effect of the phase difference between the separated oscillating fields. The shift in the hfs proved to be on the order of 120 cps, which was of the same order as the frequency errors. The experimental data obtained on the Li^6 direct transition are also shown. The curves indicated are the least-squares fit to the data obtained. For Li^6, the $\nu_{\min}$ is 215.15400(8) Mc/sec, and therefore $\Delta\nu_6=228.20528(8)$ Mc/sec. For Li^7, $\nu_{\min}$ is 695.85491 (40) Mc/sec, and therefore $\Delta\nu_7=803.50404(48)$ Mc/sec. The errors quoted are four times the statistical errors.

The hyperfine-structure anomaly between the isotopes Li^6 and Li^7 is defined as

$$\Delta_{67}=1-\frac{\Delta\nu_7 g_6}{\Delta\nu_6 g_7}\left(\frac{2I_6+1}{2I_7+1}\right)\left(\frac{\mathfrak{M}_6}{\mathfrak{M}_7}\right)^3, \qquad (5)$$

where $\mathfrak{M}$ is the reduced mass of the isotope in question. Using the ratio of the g_I values obtained by Klein,[8] $g_7/g_6=2.64090588(20)$, we obtain for the hyperfine-structure anomaly of the isotopes Li^6 and Li^7 the value $\Delta_{67}=+1.065(6)\times10^{-4}$, where the quoted error is four times the statistical error.

[8] Melvin Klein (private communication). A partial description of this experiment is given by M. P. Klein and D. F. Abell, Bull. Am. Phys. Soc. 5, 74 (1960).